Electronic Supplementary Material (ESI) for Journal of Materials Chemistry A.

Supporting Information

$Na_3V_2(PO_4)_2F_3$-SWCNT: A High Voltage Cathode for Non-aqueous and Aqueous Sodium-ion Batteries

Shuang Liu, [a] Liubin Wang, [a] Jian Liu, [a] Meng Zhou, [a] Qingshun Nian, [a] Yazhi Feng, [a] Zhanliang Tao,*[a] Lianyi Shao *[b]

[a]: Key Laboratory of Advanced Energy Materials Chemistry (Ministry of Education), College of Chemistry, Nankai University, Tianjin 300071, (P. R. China). *E-mail: taozhl@nankai.edu.cn.

[b]: School of Materials and Energy, Guangdong University of Technology, Guangzhou 510006, Guangdong, (P. R. China). *E-mail: shaolianyi@gdut.edu.cn.

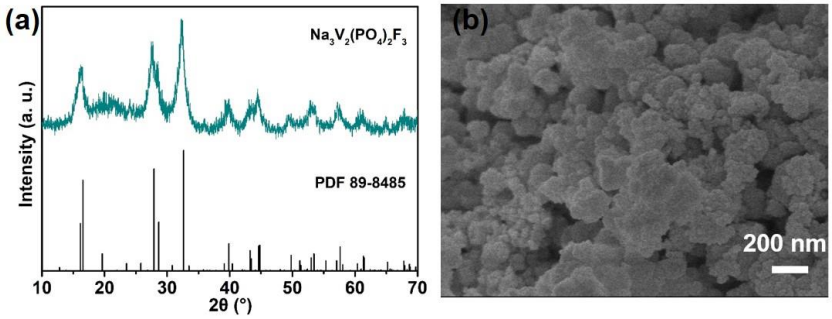

Fig. S1 (a) XRD pattern, and (b) the SEM image of pure $Na_3V_2(PO_4)_2F_3$.

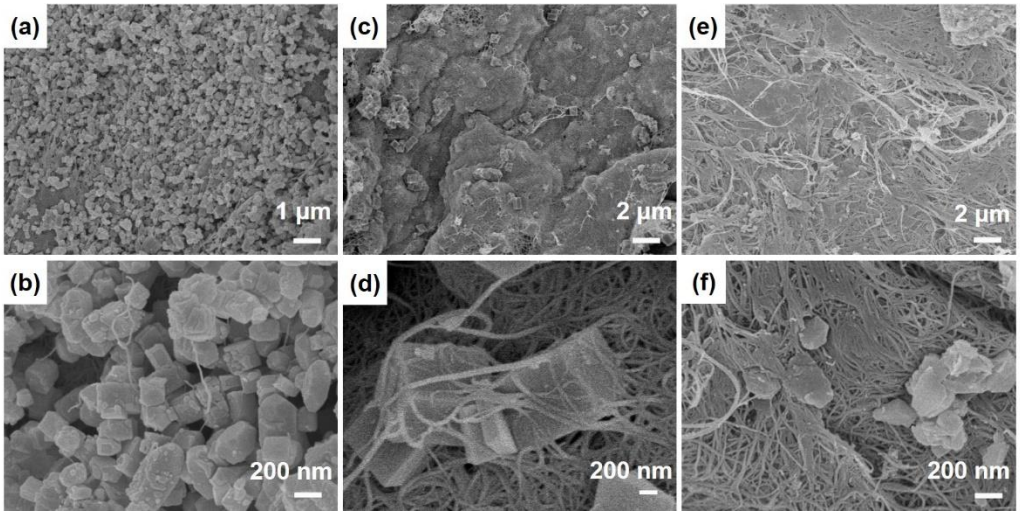

Fig. S2 The SEM images of $Na_3V_2(PO_4)_2F_3$-SWCNT-1 (a, b), $Na_3V_2(PO_4)_2F_3$-SWCNT-2 (c, d),and $Na_3V_2(PO_4)_2F_3$-SWCNT-3 (e, f).

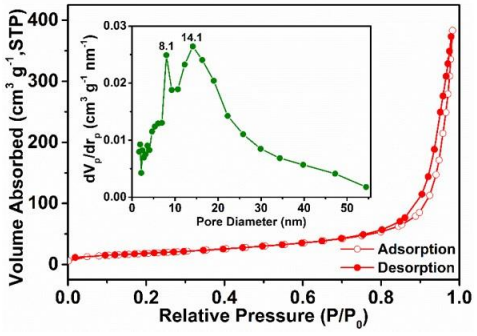

Fig. S3 N_2 adsorption and desorption isotherm of $Na_3V_2(PO_4)_2F_3$-SWCNT-2. (inset: pore-size distribution curves).

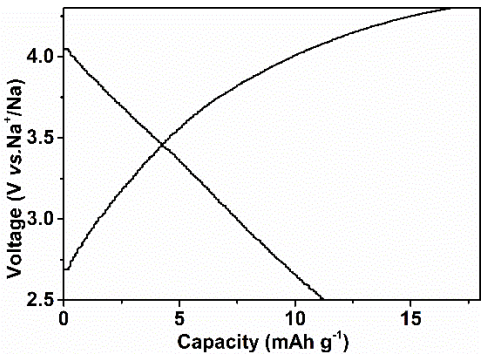

Fig. S4 Charge/discharge curves at 64 mA g^{-1} of SWCNT electrode in non-aqueous electrolyte.

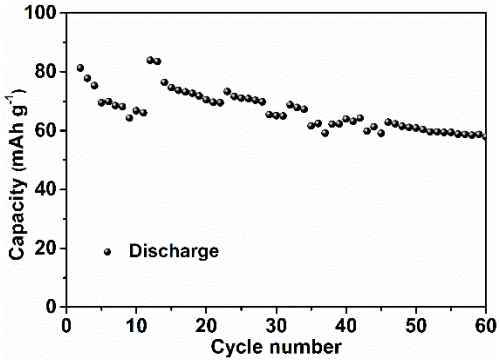

Fig. S5 The cycle performance of $Na_3V_2(PO_4)_2F_3$-SWCNT-2 electrode in 17 m $NaClO_4$ aq..

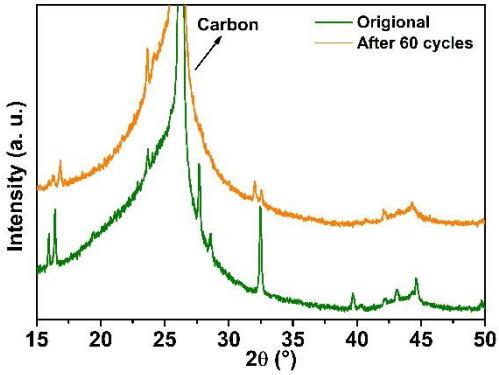

Fig. S6 XRD spectra for pristine $Na_3V_2(PO_4)_2F_3$-SWCNT-2 electrode before cycle (green line) and $Na_3V_2(PO_4)_2F_3$-SWCNT-2 electrode after 60 cycles (orange line) at 1 C in 17 m $NaClO_4$ aq..

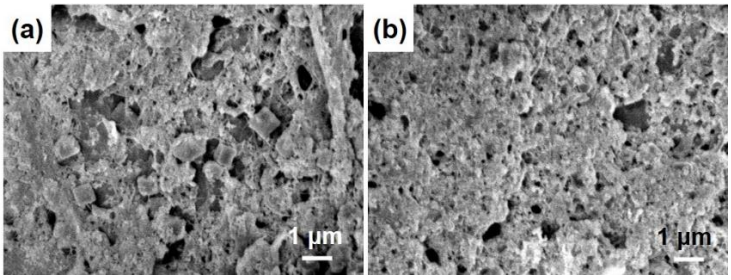

Fig. S7 SEM images for (a) pristine $Na_3V_2(PO_4)_2F_3$-SWCNT-2 electrode before cycle, (b) $Na_3V_2(PO_4)_2F_3$-SWCNT-2 electrode after 60 cycles at 1 C in 17 m $NaClO_4$ aq..

Fig. S6† shows the XRD patterns of pristine $Na_3V_2(PO_4)_2F_3$-SWCNT-2 electrode before cycle and $Na_3V_2(PO_4)_2F_3$-SWCNT-2 electrode after 60 cycles. The results show that some main characteristic peaks (16.02 °, 16.52 °, 27.76 °, 28.68 °, 39.76 °, 49.75 °) weaken after 60 cycles, resulting from the structure degradation and/or the formation of

amorphous crystal. Meanwhile, SEM results demonstrate that compared with the regular morphology of pristine $Na_3V_2(PO_4)_2F_3$-SWCNT (Fig. S7a†), the cuboids crack into particles after 60 cycles (Fig. S7b†). These phenomena suggests the degradation of $Na_3V_2(PO_4)_2F_3$-SWCNT-2.

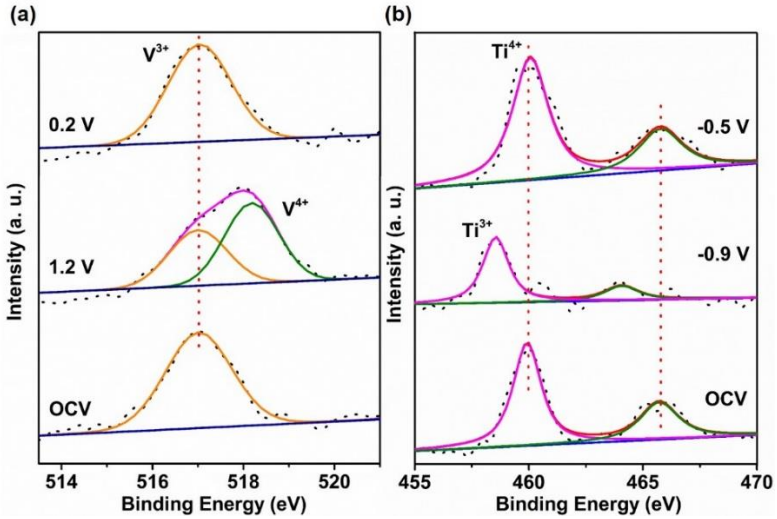

Fig. S8 XPS spectra of (a) V $2P_{3/2}$ of the $Na_3V_2(PO_4)_2F_3$-SWCNT electrode, (b) Ti $2P_{3/2}$ of the $NaTi_2(PO_4)_3$-MWCNT electrode at different charge-discharge stages in 17 m $NaClO_4$ aq..

Fig. S8a illustrates the change of vanadium valence state. Compared with the V^{3+} signal (517.01 eV) at the pristine state, V^{4+} signal (518 eV) appears at the fully charged of 1.2 V. (Fig. 4b) After discharged to 0.2 V, the binding energy value changes from 518 eV for V^{4+} to 517.03 eV for V^{3+}, indicating the conversion of $V^{3+} \leftrightarrow V^{4+}$ during the cycling.[1,2] Note that the appearence of V^{3+} is due to the incomplete reaction. In order to avoid water decomposition, cut-off voltage should be set to no more than 1.2 V, which causes the incomplete reaction. For anode, as shown in Fig. S8b, the peaks at 459.2 and 464.94 eV are assigned to Ti $2p_{3/2}$ and Ti $2p_{1/2}$ of Ti^{4+} at the pristine state.[3,4] When the electrode is discharged to -0.9 V, the binding energy of the two peaks shift to lower positions of 457.7 and 463.25 eV, indicating that the valence state of the Ti is Ti^{3+}.[4] After charged to -0.5 V, the binding energy value changes from 457.7 eV for Ti^{3+} to 459.1 eV for Ti^{4+}, suggesting the high conversion of $Ti^{3+} \leftrightarrow Ti^{4+}$ during the cycling. The XPS results reveal that there exists reversible transformation between $V^{3+} \leftrightarrow V^{4+}$ for cathode and $Ti^{3+} \leftrightarrow Ti^{4+}$ for anode during the charge–discharge process.

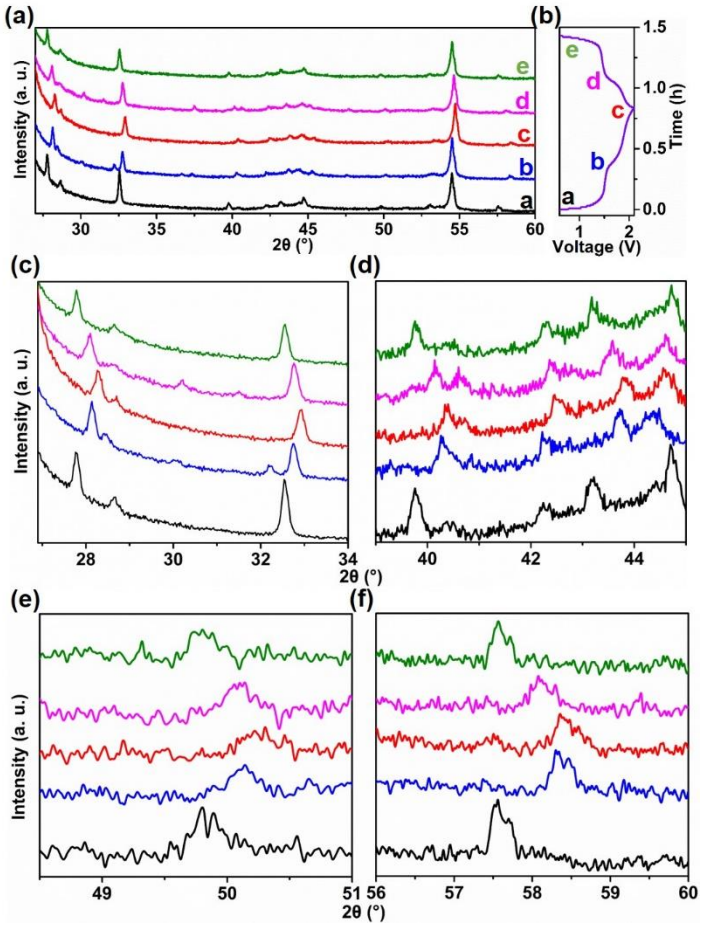

Fig. S9 (a) *Ex situ* XRD spectra collected for $Na_3V_2(PO_4)_2F_3$-SWCNT in 17 m $NaClO_4$ aq., (b) The corresponding galvanostatic charge/discharge curves of 1st cycle under 1C rate between 0.2-1.2 V. (c-f) Partial enlargement images of *ex situ* XRD profiles (The black, blue, red, purple and green lines in Fig. S9a and Fig. S9c-f are corresponding to the state of Fig. S9b, respectively).

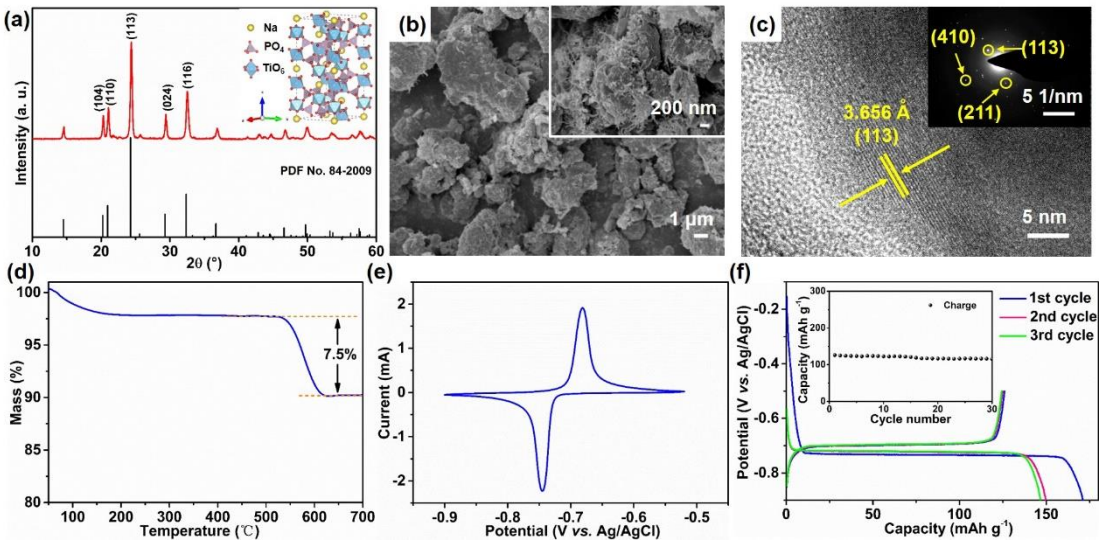

Fig. S10 (a) XRD patterns (inset: crystal structure), (b) SEM images, (c) HRTEM image (the inset is the SAED pattern), (d) TG curve, (e) CV tested at 1 mV s^{-1} and (f) charge/discharge curves at 1 C (1 C = 133 mA g^{-1}) (inset: the corresponding cyclic performance) of $NaTi_2(PO_4)_3$-MWCNT.

As displayed in Fig. S10a-b, the as-prepared $NaTi_2(PO_4)_3$-MWCNT microblocks appeare as well defined NASICON structure (JCPDS 84-2009) with aggregated particles of 2-10 μm. The clear lattice planes in HRTEM (Fig. S10c) indicates high crystallinity of the $NaTi_2(PO_4)_3$-MWCNT, and the lattice spacing of 3.656 Å can agree well with the d spacing of (113) of the $NaTi_2(PO_4)_3$-MWCNT. The corresponding SAED pattern can be indexed to the (113), (211), and (400) planes, which are attributed to the $NaTi_2(PO_4)_3$-MWCNT composite. TG curve (Fig. S10d) suggests that the carbon contents is 7.5 wt%. In addition, we also examined the electrochemical performance of $NaTi_2(PO_4)_3$-MWCNT in 17 m $NaClO_4$ aq.. CV profile in Fig. S10e is a pair of symmetrical redox peaks,which are located at −0.74 V/−0.68 V *vs.* Ag/AgCl, indicating a reversible insertion/extraction reaction of Na^+ in $NaTi_2(PO_4)_3$ lattice ($NaTi_2(PO_4)_3 + 2Na^+ + 2e^- \leftrightarrow Na_3Ti_2(PO_4)_3$). Furthermore, the redox reaction potential is much larger than the potential of H_2 evolution, water decomposition can be avoided completely. Fig. S10f shows the charge/discharge profiles of the $NaTi_2(PO_4)_3$-MWCNT anode at 1 C (1 C = 133 mAh g^{-1}). It deliveres a high charge capacity of 125 mAh g^{-1}, and a best cycle stability. What's more, the charge/discharge curves are with very long and flat plateau, suggesting an electrochemical reversibility and rapid kinetics for Na^+ in the $NaTi_2(PO_4)_3$ anode.

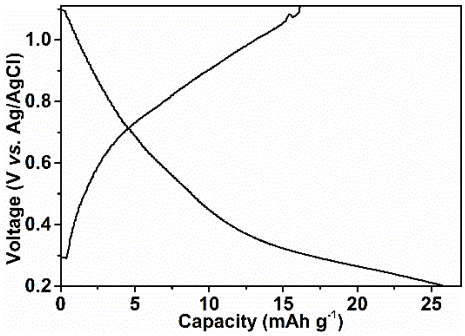

Fig. S11 (a) Charge/discharge curves at 128 mA g^{-1} of SWCNT electrode in 17 m $NaClO_4$ aq.

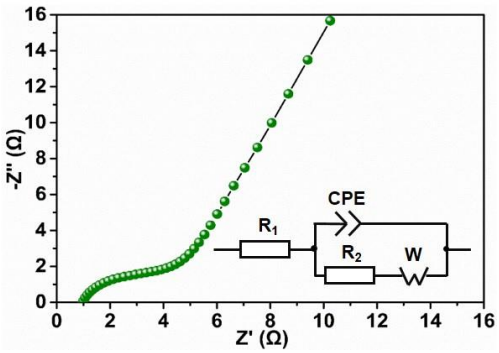

Fig. S12 Nyquist plots of $Na_3V_2(PO_4)_2F_3$-SWCNT//$NaTi_2(PO_4)_3$-MWCNT aqueous full-cell in 17 m $NaClO_4$ aq..

Notes and references

1 Y.S. Cai, X.X. Cao, Z.G. Luo, G.Z. Fang, F. Liu, J. Zhou, A.Q. Pan and S.Q. Liang, *Adv. Sci.,* 2018, 1800680.
2 C. Shen, H. Long, G.C. Wang, W. Lu, L. Shao and K.Y. Xie, *J. Mater. Chem. A,* 2018, **6,** 6007.
3 S. Liu, L.Y. Shao, X.J. Zhang, M. Zhou, Z.L. Tao and J. Chen, *J. Alloy. Compd.,* 2018,**754,** 147.
4 R.L. Kurtz and V.E. Henrich, *Surf. Sci. Spectra,* 1998, **5,** 179.